

A WOLF IN SHEEPSKIN: EXTRAORDINARY SUPERNOVA 2012AU VEILED BEHIND ORDINARY RADIO EMISSION

ATISH KAMBLE¹, ALICIA M. SODERBERG¹, LAURA CHOMIUK^{2,3,4}, RAFFAELLA MARGUTTI¹, MIKHAIL MEDVEDEV^{5,6}, SAYAN CHAKRABORTI¹, ROGER CHEVALIER⁷, NIKOLAI CHUGAI⁸, JASON DITTMANN¹, MARIA DROUT¹, CLAES FRANSSON⁹, DAN MILISAVLJEVIC¹, EHUD NAKAR¹⁰, NATHAN SANDERS¹

Draft version April 20, 2022

ABSTRACT

We present extensive radio and X-ray observations of SN 2012au, the energetic radio luminous supernova of type Ib that may be a link between subsets of hydrogen-poor superluminous and normal core-collapse supernovae. The observations closely follow models of synchrotron emission from shock heated circum-burst medium that has a wind density profile ($\rho \propto r^{-2}$). We infer a sub-relativistic velocity for the shock wave $v \approx 0.2c$ and a radius of $r \approx 1.4 \times 10^{16}$ cm at 25 days after the estimated date of explosion. For a constant wind velocity of 1000 km/s we determine the constant mass loss rate of the progenitor to be $\dot{M} = 3.6 \times 10^{-6} M_{\odot} \text{ yr}^{-1}$, consistent with the estimates from X-ray observations. We estimate the total internal energy of the radio emitting material to be $E \approx 10^{47}$ erg, which is intermediate to SN 1998bw and SN 2002ap. Evolution of the radio light curves of SN 2012au is consistent with interaction with a smoothly distributed circum-burst medium and absence of stellar shells ejected from previous outbursts out to $r \approx 10^{17}$ cm from the supernova site. Based on this we conclude that the evolution of the SN 2012au progenitor star was relatively quiet during the final years preceding explosion. We find that the bright radio emission from SN2012au was not dissimilar from other core collapse supernovae despite its extraordinary optical properties. We speculate that it was the nature of the explosion that led to the unusual demise of the SN2012au progenitor star.

Subject headings: radiation mechanisms: nonthermal - radio continuum: general - supernovae: general - supernovae: individual (SN 2012au)

1. INTRODUCTION

Optical studies have recently discovered a new class of supernovae – Super Luminous Supernovae (SLSNe) with absolute magnitude of ≤ -21 (Quimby et al. 2011; Gal-Yam 2012). Models of SLSNe suggest very massive progenitors $M > 70 M_{\odot}$ which undergo dynamical instability due to the formation of $e^{-} - e^{+}$ pairs (Barkat et al. 1967). The recent discovery and follow-up data for SN 2012au reveals several features of SLSNe in the optical light curve and spectral evolution, as shown by Milisavljevic et al. (2013a); Takaki et al. (2013), which suggests it to be a link in the chain: the normal core collapse supernovae \rightarrow hypernovae \rightarrow SLSNe. Such explosive events have been suggested to have pre-explosion pair-instability eruptions (Chatzopoulos & Wheeler 2012) creating shells of CSM in the vicinity of the SN progeni-

tor system. Radio emission from supernovae serves as a probe of the circum-burst environment through the excitation of local particles to relativistic velocities (Weiler et al. 2002) and may therefore be used to search for CSM shells. Although a few candidate SLSNe have been tried (Chomiuk et al. 2011), to date there has been no radio detection of a SLSN. This makes SN 2012au a potential first look at the mass loss properties of a SLSN.

In this article, we report radio and X-ray observations and analysis of SN 2012au, and show that it had a radio luminosity and associated energy intermediate between the broad-lined and energetic type Ic SNe 2002ap and 1998bw. SN 2012au points to the existence of a population of supernovae occupying the phase space between normal and relativistic core collapse supernovae. The organization of this paper is as follows: Radio observations using the Jansky Very Large Array (VLA) and X-ray observations from *Swift* X-ray Telescope (XRT) are described in Section 2.1 and 2.2, respectively. Preliminary estimates of the physical parameters governing the explosion and radiation, based on the assumption of equipartition, are obtained in Section 3. In Section 4 we present detailed analysis and resultant parameters without the equipartition assumption. The inverse Compton X-ray emission from SN 2012au is discussed in Section 5 and then we try to constrain the microphysical parameters ϵ_e and ϵ_B in Section 6. We discuss implications of SN 2012au in regards to different models such as Pair Instability Supernovae (PISN) and Pulsational Pair Instability Supernovae (PPISN) (7.1), and compare it with other energetic SNe Ib/c (7.2) and also the possibility of it being asymmetric (7.3). Comparison with other SNe

¹ Harvard-Smithsonian Center for Astrophysics, 60 Garden St., Cambridge, MA 02138

² Department of Physics and Astronomy, Michigan State University, East Lansing, MI 48824, USA

³ National Radio Astronomy Observatory, P.O. Box O, Socorro, NM 87801, USA

⁴ Jansky Fellow

⁵ the Department of Physics and Astronomy, University of Kansas, Lawrence, KS 66045, USA

⁶ the ITP, NRC Kurchatov Institute, Moscow 123182, Russia

⁷ Department of Astronomy, University of Virginia, P.O. Box 400325, Charlottesville, VA 22904-4325, USA

⁸ Institute of Astronomy, Russian Academy of Sciences, Pyatnitskaya 48, 109017 Moscow, Russia

⁹ Department of Astronomy, The Oskar Klein Centre, Stockholm University, AlbaNova University Centre, SE-106 91 Stockholm, Sweden

¹⁰ Raymond and Beverly Sackler School of Physics and Astronomy, Tel Aviv University, Tel Aviv 69978, Israel

TABLE 1
VLA RADIO FLUX DENSITY MEASUREMENTS OF SN 2012AU

Date (UT)	MJD	Frequency (GHz)	$F \pm \sigma$ (mJy)	Array Config.
2012 Mar 20.2	56006.2	5.0	4.596 ± 0.025	C
...	...	6.75	7.294 ± 0.019	...
2012 Mar 24.3	56010.3	4.55	5.658 ± 0.036	C
...	...	7.45	10.113 ± 0.020	...
...	...	13.3	9.709 ± 0.049	...
...	...	16.0	8.408 ± 0.058	...
...	...	29.0	3.778 ± 0.072	...
...	...	37.0	2.772 ± 0.098	...
2012 Apr 23.1	56040.1	2.5	7.900 ± 0.142	C
...	...	3.5	9.886 ± 0.053	...
...	...	4.55	9.569 ± 0.052	...
...	...	7.45	6.630 ± 0.024	...
...	...	13.3	3.446 ± 0.040	...
...	...	16.0	2.843 ± 0.034	...
2012 May 21.1	56068.1	13.3	2.049 ± 0.034	CnB
...	...	16.0	1.662 ± 0.032	...
2012 Jun 23.0	56101.0	13.3	1.079 ± 0.049	B
...	...	16.0	0.797 ± 0.050	...

in energy-velocity phase space is discussed in Section 7.4. Our conclusions are summarized in Section 8.

2. OBSERVATIONS

2.1. Radio Observations using Very Large Array

SN 2012au was optically discovered on 14 March 2012 by the CRTS SNHunt project, with an offset of about $3''.5$ E and $2''.0$ N from the center of the host galaxy NGC 4790 (Howerton et al. 2012) at a distance of $d \approx 23.5$ Mpc (Theureau et al. 2007). In our first observation with the VLA¹¹ on 2012 March 20.2 UT, we detected a bright radio source coincident with the optical position at $\alpha(\text{J2000}) = 12^{\text{h}}54^{\text{m}}52.18^{\text{s}}$ and $\delta(\text{J2000}) = -10^{\circ}14'50.2''$ (± 0.1 arcsec in each coordinate) with flux density of $f_{\nu} = 4.59 \pm 0.025$ mJy at 5 GHz. This, and subsequent observations from 5 to 37 GHz, are summarized in Table 1.

All observations were taken in standard continuum observing mode with a bandwidth of 16×64 MHz. During the reduction we split the data in two side bands (8×64 MHz) of approximately 1 GHz each. We used 3C286 for flux calibration, and for phase referencing we used calibrators J1305-1033. Data were reduced using standard packages within the Astronomical Image Processing System (AIPS).

The radio spectral energy distribution (SED) of SN 2012au as observed on March 24 and April 23, 2012 are shown in Figure 1. In the optically thin regime we measure $f_{\nu} \propto \nu^{-0.85 \pm 0.02}$. Figure 2 shows the SN 2012au radio light-curves assuming an approximate explosion date of 2012 March 3.5 UT (MJD 55990.5 ± 2.0) following Milisavljevic et al. (2013a).

2.2. X-ray Observations using Swift

We observed SN 2012au with the *Swift* (Gehrels et al. 2004) X-Ray Telescope (XRT, Burrows et al. 2005) starting from 2012 March 15 until 2012 April 21, or roughly

¹¹ The Jansky Very Large Array is operated by the National Radio Astronomy Observatory, a facility of the National Science Foundation operated under cooperative agreement by Associated Universities, Inc.

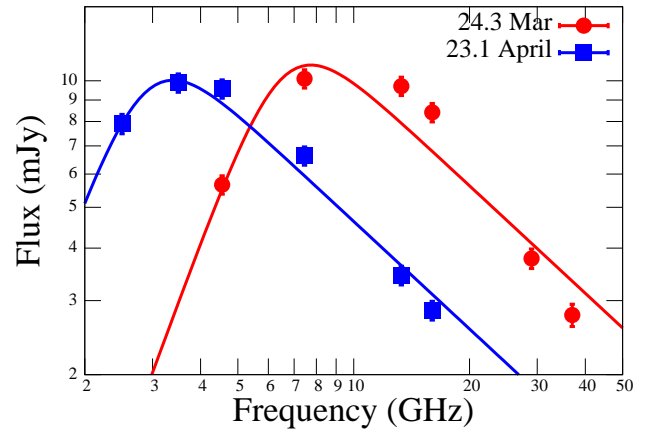


FIG. 1.— Radio SED of SN 2012au on 24.3 March and 23.1 April 2012, about 21 and 51 days after the supernova, respectively.

between 12 and 48 days since the supernova. Data have been reduced with HEASoft v. 6.13 and corresponding calibration files. Standard filtering and screening criteria have been applied. Using a total of 34.7 ks, we find evidence for significant X-ray emission at a position consistent with SN 2012au, with 0.3-10 keV count-rate of $(11.6 \pm 2.5) \times 10^{-4} \text{ c s}^{-1}$ corresponding to a 4.6σ detection. Adopting a simple power-law spectrum and correcting for the Galactic absorption in the direction of SN 2012au ($\text{NH}_{\text{MW}} = 3.7 \times 10^{20} \text{ cm}^{-2}$, Kalberla et al. 2005), the measured count-rate translates into an unabsorbed flux of $(4.6 \pm 1.0) \times 10^{-14} \text{ erg s}^{-1} \text{ cm}^{-2}$ ($L_X \sim 3 \times 10^{39} \text{ erg s}^{-1}$).

SN 2012au is positioned at less than $10''$ far from the center of NGC4790's central nucleus (Milisavljevic et al. 2013a, their Fig. 1). The Half Energy Width (HEW) of *Swift*-XRT is $\sim 18''$ (for an on-axis source at 1.5 keV, Moretti et al. 2005) thus, X-ray emission from the host nucleus might contaminate the detected X-ray emission. However, splitting the data set into two halves with exposure times of 9.8 ks and 24.9 ks, respectively, and applying a binomial test, we find evidence for fading of the X-ray emission, with a probability of a chance fluctuation of 0.7%. The detection of fading on a time-scale of ~ 30 days suggests that SN 2012au dominates the X-ray emission we detect. In the following we proceed with this hypothesis.

3. PRELIMINARY CONSTRAINTS FROM EQUIPARTITION ASSUMPTION

Radio observations of supernovae primarily trace the shocked ejecta and have proven to be a good probe of the velocity of the shock wave and kinetic energy of the ejecta. To first degree approximation these quantities can be estimated quickly, without detailed observations, using the reasonable assumption of energy equipartition between magnetic field (ϵ_B) and accelerated electrons (ϵ_e). Under the assumption of equipartition ($\epsilon_e = \epsilon_B = 0.5$) the angular radius of the shock wave, θ_{ep} , and the equipartition energy, E_{ep} , are given by

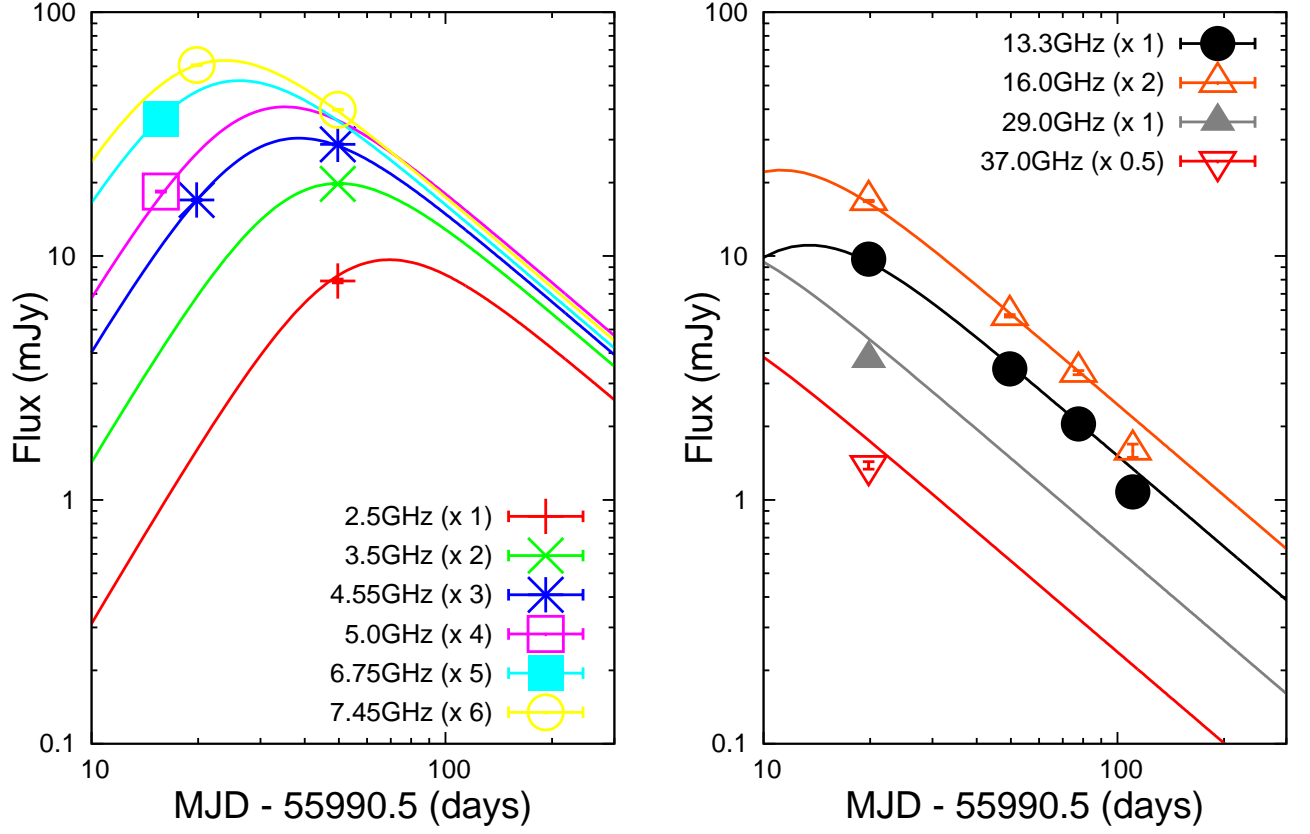


FIG. 2.— Radio light curves of type Ic SN 2012au as observed with the VLA at frequencies from 2.5 GHz to 37 GHz between March 20 and June 23, 2012. The model light curves, i.e. synchrotron self-absorbed radiation from the non-relativistic freely expanding blast wave interacting with the wind stratified medium, have been over plotted the data points. Both, the model light curves and the data points, have been off-set for the purpose of clarity.

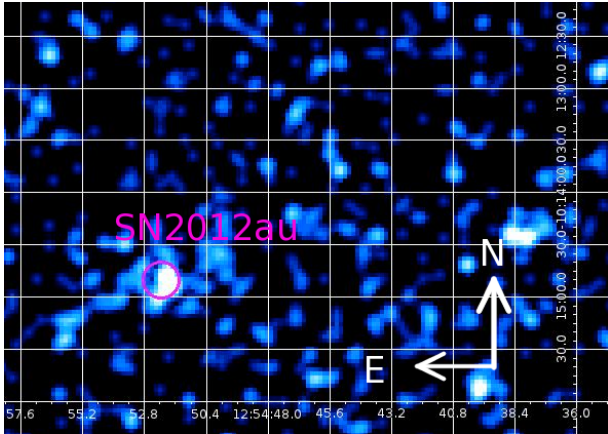


FIG. 3.— *Swift* X-ray image of SN2012au

$$\theta_{ep} \approx 120 \left(\frac{d_L}{\text{Mpc}} \right)^{-1/17} \left(\frac{f_{\nu_a}}{\text{mJy}} \right)^{8/17} \left(\frac{\nu_a}{\text{GHz}} \right)^{-(36-p)/34} \mu\text{as} \quad (1)$$

$$E_{ep} \approx 4 \times 10^{43} \left(\frac{d_L}{\text{Mpc}} \right)^{40/17} \left(\frac{f_{\nu_a}}{\text{mJy}} \right)^{20/17} \left(\frac{\nu_a}{\text{GHz}} \right)^{-(3p+11)/17} \text{erg} \quad (2)$$

following Chevalier (1998); Kulkarni et al. (1998) and Soderberg et al. (2005). Using our VLA observation of SN 2012au on 24.3 March 2012 ($t = 20.8$ days), we find that the self-absorption frequency $\nu_a \approx 8$ GHz, corresponding flux $f_{\nu_a} \approx 10$ mJy and $p \approx 2.7$. Using equations 1 and 2, these parameters give energy $E_{ep} \approx 10^{47}$ erg and the angular size of the shock wave $\theta_{ep} \approx 39 \mu\text{arcsec}$. At a distance $d_L \approx 23.5$ Mpc, this size translates to

the equipartition radius of $r_{ep} \approx 1.4 \times 10^{16}$ cm and the expansion velocity $v \equiv \beta c \approx 0.26c$. Most core-collapse supernovae have $\beta \approx 0.1 - 0.15$ (see e.g. Chevalier & Fransson 2006; Soderberg et al. 2010) which makes this a relatively faster supernova shock wave.

4. RADIO LUMINOSITY AND SYNCHROTRON SELF-ABSORPTION

Although equipartition arguments provide reasonable estimates of the important physical parameters that drive the explosion and its evolution, it is far from clear if the equipartition holds in general for supernova blast-waves or if it sets in at a particular stage during the evolution. Therefore, to do away with the assumption of equipartition and to treat the supernovae in general, in the Appendix we have developed a formulation of SN blast-wave driven synchrotron radiation and its evolution following Chevalier (1998); Soderberg et al. (2005); Chevalier & Fransson (2006).

Consider a shock wave expanding into the circum-burst medium with velocity β , expressed in units of the speed of light. The size and speed of the shock wave evolve in time as

$$r = r_0(t/t_0)^m \quad (3)$$

$$\beta = \beta_0(t/t_0)^{m-1} \quad (4)$$

where $\beta c = dr/dt$ and the subscript ‘0’ refers to quantities measured at epoch t_0 . The circum-burst medium is assumed to be of wind profile, $n(r) \propto r^{-2}$. The synchrotron emission from SN blast-waves peak at radio frequency bands. The observed multiband spectral energy distribution due to a SN blast-wave could be characterized by three observables: two break frequencies (ν_m and ν_a) and the spectral peak flux (f_{ν_a}). As the break frequencies evolve in time, flux measured at a given fixed frequency changes smoothly resulting in a light curve. The complete evolution of the blast-wave could be described by four independent physical parameters: expansion velocity of the blast wave β , fractional energy deposited in the relativistic electrons (ϵ_e) & in the magnetic field (ϵ_B), and the circum-burst density into which the blast-wave is expanding $n(r)$ which could also be written either as a wind parameter A_\star or the mass loss rate of the star \dot{M} as defined in the Appendix. Also we define $\epsilon_f = \epsilon_e/\epsilon_B$. The situation $\epsilon_f = 1$ corresponds to equipartition i.e., the equal amount of fractional energy in accelerated electrons and magnetic fields. Equations A13, A14 and A15 could then be inverted to get physical parameters of the explosion in terms of the observables.

$$\beta_0 = 0.18 m d_{L,100}^{16/17} f_{\nu_a, mJy}^{8/17} \nu_{a,10}^{-33/34} \nu_{m,7}^{-1/34} t_{0,d}^{-m} \epsilon_f^{-1/17} \quad (5)$$

$$A_\star = 0.65 d_{L,100}^{22/17} f_{\nu_a, mJy}^{11/17} \nu_{a,10}^{29/34} \epsilon_f^{5/17} \nu_{m,7}^{-29/34} \quad (6)$$

$$\epsilon_B = 0.29 m^{-2} \nu_{a,10}^{47/34} \nu_{m,7}^{21/34} t_{0,d}^2 d_{L,100}^{-30/17} f_{\nu_a, mJy}^{-15/17} \epsilon_f^{-13/17} \quad (7)$$

The numerical coefficients are the results of particular choice of units of the observables: f_{ν_a} in mJy, ν_a in 10^{10} Hz, ν_m in 10^7 Hz, t_0 in days and distance d_L in 100 Mpc.

4.1. Model Fits, Spectral and Physical Parameters

To fit all the radio observations collectively we used the smooth broken power law

$$f_\nu(\nu, t) = f_{a,0} \times \left[\left(\frac{\nu}{\nu_a(t)} \right)^{-\alpha_1 s} + \left(\frac{\nu}{\nu_a(t)} \right)^{-\alpha_2 s} \right]^{-1/s} \quad (8)$$

where $\alpha_1 = 5/2$ and $\alpha_2 = -(p-1)/2$ are the standard synchrotron self-absorption and optically thin spectrum scenario, respectively, for the power law distribution of electrons (Eqn. A1) with index p . Further in this prescription $f_{a,0} \equiv f_\nu(\nu = \nu_a, t = t_0)$ i.e. spectral peak is measured at the self-absorption frequency and at epoch $t = t_0$. The parameter ‘s’ in Eqn.8 is the smoothing parameter - higher value of s leads to sharper break compared to that with the lower s .

The statistical uncertainties in fluxes measured and listed in Table 1 are the image RMSs. Variations in the local weather at the telescope can introduce additional errors to the measured image RMSs. Furthermore, calibration of the flux and phase calibrators can add systematic errors of a few percentage. Therefore, during the model fitting, about 5% of the total error was added in quadrature to account for these sources of errors.

Milislavjevic et al. (2013a) has determined the epoch of explosion for SN 2012au to be March 3.5 ± 2.0 based on the optical photometry. We used the same epoch of explosion for our fitting of the radio data. The radio SED indicate that frequency $\nu_m < \nu_a$ during all the observations and in any case below the observing frequency ν_{obs} . As a result, we can constrain the spectral break $\nu_m < 1$ GHz.

We fit the multifrequency light curves of SN 2012au to the model described in the appendix by using least square minimization to estimate the self-absorption frequency (ν_a) and spectral peak (f_{ν_a}). The best fit values turned out to be $f_{\nu_a} = 14.6 \pm 0.3$ mJy at the self-absorption frequency $\nu_a = 6.0 \pm 0.1$ GHz at the epoch of $t_0 = 25$ days after the burst and the resultant $\chi^2/\text{dof} = 9$. We note that a significant contribution to the χ^2 comes from the observations at high-frequencies (> 8 GHz).

The shock wave expansion is best fit as $r = r_0(t/t_0)^{0.93}$. For a compact, radiative envelope star, the outer density profile should tend to a power law, $\rho_{sn} \propto r^{-k}$ with $k \sim 10.2$ (Chevalier & Fransson 2006). For a wind medium, the shock front expands as $r \propto t^m$, with $m = (k-3)/(k-2)$, so $k = 0.88$ is expected. Our estimate $m = 0.93$ from the radio model, is therefore in a reasonable agreement.

We left p as well as ‘s’ as free parameters to allow for the best match with the radio spectra as well as light curves. The fit converged to $p = 2.7 \pm 0.1$ and $s = 1.9 \pm 0.2$. The best fit value of p thus found is close to the typical values ($p \approx 3$) found for SNe Ibc (Chevalier & Fransson 2006).

At this stage we do not assume any particular value for ϵ_e or effectively for ϵ_f . Using our best fit spectral parameters for SN 2012au and equations 5-7 we determined $\beta_0 = 0.20 \epsilon_f^{-1/17}$, $A_\star = 0.4 \epsilon_f^{5/17}$ and $\epsilon_B = 0.3 \epsilon_f^{-13/17}$.

The size of the supernova shock wave at epoch $t_0 = 25$ days is thus $r_0 = \beta_0 c t_0 / m$ which from the derived quantities is estimated to be $r_0 = 1.4 \times 10^{16} \epsilon_f^{-1/17}$ cm. As could be seen both the quantities β and r have a rather weak dependence on the parameter ϵ_f .

The value of ϵ_B could now be converted to the shock compressed magnetic field $B = 0.54\epsilon_f^{-4/17}$ G. Similarly, the minimum Lorentz factor of electron energy distribution turns out to be $\gamma_m = 2.6\epsilon_f^{2/17}$. This estimate is consistent with our assumption that the radiating electrons are relativistic, with the spectrum extending down to $\gamma_m > 1$. Although γ_m has a weak dependence on ϵ_f a very low value of ϵ_f or ϵ_e leading to $\gamma_m < 1$ would not be sensible.

The mass loss rate of the progenitor star is defined as $\dot{M} = 5 \times 10^{11} 4\pi V_w A_* \text{ gm cm}^{-1}$ for the constant wind velocity $V_w = 1000 \text{ km/s}$ and normalization A_* . For the derived value of A_* this gives, $\dot{M} = 3.6 \times 10^{-6} \epsilon_f^{5/17} M_\odot \text{ yr}^{-1}$. We note that this estimated mass loss rate is approximately a factor of 10 and 20 higher than that of SN 2002ap and SN 1998bw, respectively. This value is still at the lower end of the range of typical values found for the Wolf-Rayet stars (Cappa et al. 2004) which are considered to be the candidate progenitors of typical type Ib/c SNe as well as GRBs.

The density profile of the circum-burst material is consistent with a steady wind due to constant mass loss rate and constant wind velocity. We can also estimate the number density of the wind at a distance r from the progenitor to be:

$$n_e = \frac{B_0^2 p - 2}{8\pi p - 1} \frac{\epsilon_f}{4m_e c^2 \gamma_{m,0}} \left(\frac{r}{r_0}\right)^{-2} \quad (9)$$

For the measured physical parameters, we find $n_e \approx 9 \times 10^2 (r/r_0)^{-2} \text{ cm}^{-3}$.

Perhaps the most important physical parameter, the total internal energy for the radio emitting material can now be estimated with

$$E = \frac{4\pi r_0^3}{\eta} \frac{1}{\epsilon_B} \frac{B_0^2}{8\pi} \left(\frac{r}{r_0}\right)^{-2}, \quad (10)$$

which yields a value of $E = 6 \times 10^{46} \epsilon_f^{2/17} \text{ erg}$ at the epoch of $t_0 = 25$ days. This estimated energy is intermediate between that of the two hypernovae - about 100 times lower than SN 1998bw and about 100 times higher than SN 2002ap.

Although the model in its current form does not take into account geometric effects, such as collimation or asymmetry, it does provide reasonable fits to the observations and large deviations from true physical parameters are unlikely.

5. INVERSE COMPTON X-RAY EMISSION

The interaction of the SN shock with the circumstellar medium (CSM) is a well known source of X-ray radiation (Björnsson & Fransson 2004, Chevalier & Fransson 2006). Monitoring the high-energy emission from SNe therefore allows us to map the mass-loss history of the progenitor in the years before the explosion. In the case of hydrogen-stripped SNe exploding in low density environments, Björnsson & Fransson (2004) and Chevalier & Fransson (2006) demonstrated that the dominant X-ray emission mechanism during the first weeks to a month after the explosion is Inverse Compton (IC). In this framework, X-ray photons originate from the up-scattering of

optical photons from the SN photosphere by a population of electrons accelerated to relativistic speeds by the SN shock.

Following Chevalier & Fransson (2006), the IC X-ray luminosity depends on: (i) the density structure of the SN ejecta (ii) and of the CSM; (iii) the details of the electron distribution responsible for the up-scattering; (iv) the explosion parameters (ejecta mass M_{ej} and kinetic energy E_k); and (v) the bolometric luminosity of the SN ($L_{IC} \propto L_{bol}$). As inferred from the radio observations we assume wind medium and an electron power-law index $p = 2.7$. From the modeling of the bolometric light-curve, Milisavljevic et al. (2013a) constrained the ejecta mass and kinetic energy to be $M_{ej} \sim 4 M_\odot$ and $E_k = 10^{52} \text{ erg}$. Using these parameters and the formalism developed by Margutti et al. (2012), the *Swift*-XRT observations constrain the mass-loss rate from the progenitor to $\dot{M} \sim 5.6 \times 10^{-6} \times \epsilon_{e,0.1}^{-2.39} M_\odot \text{ yr}^{-1}$, consistent with radio measurements, where $\epsilon_{e,0.1}$ is the fraction of energy into relativistic electrons in units of 0.1 and we assumed a wind velocity of $V_w = 1000 \text{ km s}^{-1}$.

One can further use independent estimates of mass loss rates from radio and X-ray emissions to constrain fractions of energy in accelerated electrons and magnetic field. As can be seen, \dot{M} from X-rays depends strongly on ϵ_e while that from radio, has a weak dependence on both ϵ_e and ϵ_B . Equating those mass-loss rates, we constrain $\epsilon_e = 0.15 \epsilon_B^{0.11}$. These quantities can be constrained rather strongly by alternative means as shown in the next section.

6. CONSTRAINTS ON ϵ_E AND ϵ_B

In the previous section we used $\nu_m < 1 \text{ GHz}$ and, in the absence of forth observable, expressed all the results in terms of ϵ_f . In this section we will relax the assumption about ν_m and will try to constrain ϵ_f .

For simplicity, it is often assumed that $\epsilon_f = 1$ which translates to $\epsilon_e = \epsilon_B$ or equipartition of energy between accelerated electrons and shocked magnetic field. In general, however, ϵ_f could have any non-zero positive value. By combining equations 5 and 7, we can eliminate ν_m between them and using the observed spectral parameter values for ν_a and f_{ν_a} one obtains

$$\beta_0 = \frac{0.24}{\epsilon_B^{1/21} \epsilon_f^{2/21}} \quad (11)$$

In Figure 4, we show the $\beta - \epsilon_B$ phase-space with contours corresponding to two different values of ϵ_f , viz., $\epsilon_f = 1$ and $\epsilon_e + \epsilon_B = 1$. The restricted or highly unlikely values are marked by shaded green and orange regions.

As discussed before $\epsilon_f = 1$ corresponds to the energy equipartition between shocked electrons and magnetic field. The green shaded region is $\epsilon_f < 1$ or equivalently $\epsilon_e < \epsilon_B$. Observations of SNe, supernova remnants and GRBs suggest that usually $\epsilon_e > \epsilon_B$. On the other hand, $\epsilon_e + \epsilon_B \leq 1$ condition ought to be satisfied, leaving out the orange shaded region as not-permissible.

Medvedev (2006) showed that $\epsilon_e = (\lambda/\beta)\sqrt{\epsilon_B}$ for relativistic shocks such as in the case of GRBs. The dimensionless parameter λ , which accounts for the geometry of the current filaments and other plasma effects, has been found to range from about unity to a few based on the results of numerical simulations. The results of Medvedev

(2006) should also hold for sub-relativistic shocks with a moderate value of β , because the magnetic field in the circum-burst medium (\sim a few μG) is much smaller than the shock-generated fields (\sim a few hundred mG) so that the shock structure is mediated by plasma streaming instabilities. Using this relation along with Eqn.11 gives $\beta = 0.2\lambda^{-2/19}$. The blue shaded region in Figure 4 bounds the higher and lower limits obtained for $\lambda = 0.5$ and 3, respectively. The lower value of $\lambda = 0.5$ limits the shock velocity to $\beta \leq 0.22$, which along with the condition $\epsilon_e + \epsilon_B \leq 1$ gives $\epsilon_B \leq 0.15$.

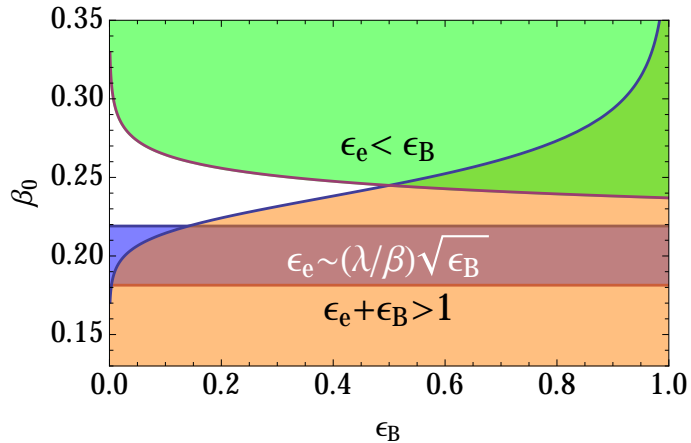


FIG. 4.— $\beta - \epsilon_B$ parameter space for SN 2012au. The green shaded region corresponds to $\epsilon_e < \epsilon_B$. The energy conservation requires that $\epsilon_e + \epsilon_B \leq 1$, ruling out the orange shaded region. The relation $\beta \propto \lambda^{-2/19}$ enclosed between $0.5 < \lambda < 3.0$ is coded in blue.

7. DISCUSSION

7.1. Shock wave interaction with the steady wind

Towards the end of their lives very massive stars ($M \gtrsim 70M_\odot$) are likely to undergo dynamical instability due to the $e^- - e^+$ pair formation leading to complete disruption of the star as a pair-instability supernova (PISN) (Barkat et al. 1967). At a lower mass range of stars favorable rotation periods and metallicities could result in episodic ejection of matter shells from the outer stellar layers but not total disruption of the star. This is called the pulsational pair-instability supernova (PPISN). Some of the most luminous supernovae are considered to have originated as PPISN and PISN, for instance, SN 2006gy (Smith et al. 2007; Ofek et al. 2007; Nomoto et al. 2007) and SN 2007bi (Gal-Yam et al. 2009; Young et al. 2010). The stellar shell ejected as a result of the ultimate core collapse and SN explosion, which would eventually take place in this modified environment, could subsequently be expected to interact with the previously ejected shells, see e.g. Chatzopoulos & Wheeler (2012). Signatures of such interactions in the form of bumpy light curves could serve as proof of a possible massive star progenitor as well as PPISN candidates.

The case has been made for SN 2012au as being a link between SLSN and normal core collapse supernovae (Milisavljevic et al. 2013a). The radio light curves of this event are smooth as shown in Figure 2. There is, therefore, no evidence of the shock wave interacting with inhomogeneous circum-burst medium out to $r \approx 10^{17}$ cm

from the supernova site. The alternative interpretation that SN 2012au was an asymmetric explosion by Milisavljevic et al. (2013a) based on spectral evolution and the two component velocity behavior implied by several spectral features is, therefore, consistent with this finding.

The lack of shock-shell interaction may also mean that there is a significant delay between the ejection of shells and the supernova thereby resulting in the shells being able to travel far away from the supernova site. Our observations suggest that the last few decades of the progenitor of SN 2012au were quiet during which no such shell ejections took place.

7.2. SN 2012au in comparison with the hypernovae

The peak bolometric luminosity of SN 2012au was about $L_{bol} \approx 6 \times 10^{42}$ erg/s, modeling of which and the overall UV-optical-NIR band light curves of SN 2012au suggest that the progenitor ejected $M_{ej} \approx 3 - 5M_\odot$ with the kinetic energy of $E_K \approx 10^{52}$ erg (Milisavljevic et al. 2013a; Takaki et al. 2013) as compared to the ordinary type Ib/c SNe which have $E_K \approx 10^{51}$ erg. This makes SN 2012au a ‘‘hypernova’’, a class which, as of now, constitutes only a few more peculiar SNe such as SN 1997ef, SN 1998bw and SN 2002ap, for instance. While a few more candidates of this class have been identified and studied in optical band, no detailed studies have been possible in the radio due to the paucity of similar detected events in the local universe. The radio bright SN 2012au therefore is a rare and important addition to this class.

Table 2 compares important explosion and environmental parameters of a few hypernovae estimated from their optical and radio evolution. SN 1998bw was a supernova associated with GRB980425, and was extraordinary for several reasons: broad-absorption features in the spectrum associated with velocities in excess of 30,000 km/s, large kinetic energy ($> 10^{52}$ erg) in the ejecta radiating in optical (slower ejecta) and a relativistic shock wave in the front powered by large kinetic energy ($> 10^{49}$ erg) leading to a bright radio emission. Similar broad absorption lines and large kinetic energy ($> 10^{52}$ erg) were inferred from the optical emission of SN 2002ap evoking excitement in the community leading to intense observing campaigns. SN 2002ap, however, turned out to be rather faint: about 1000 times fainter than its predecessor SN 1998bw, in radio emission. Detailed analysis of radio observations suggested a low reservoir of energy ($E_K \sim 10^{45}$ erg) in the high velocity ejecta leading to the conclusion that broad-absorption lines do not necessarily serve as proxy for relativistic shock waves (Berger et al. 2002).

Explosion parameters for SN 2012au, inferred from optical observations are similar to those of SN 1998bw. The peak radio brightness was, however, intermediate - ~ 10 times fainter than SN 1998bw but > 100 times brighter than SN 2002ap. While the shock wave is non-relativistic with $v \sim 0.2c$, the kinetic energy is significant, $E_K \sim 10^{47}$ erg, which is about 100 times less than SN 1998bw but larger than that of SN 2002ap by a similar factor (see Figure 5). Thus, SN 2012au occupies the intermediate space between the extremes of SN 1998bw and SN 2002ap.

The differences in the brightness of radio emission

may be traced to the mass loss histories and velocities of the shock waves. The inferred mass-loss rate for SN 2012au is at least an order of magnitude higher than both SN 1998bw and SN 2002ap. We note that the metallicity of the explosion site of SN2012au is super solar, $Z \sim 2 Z_{\odot}$. Given the mass loss and metallicity relation $\dot{M} \sim Z^{0.8}$ (Asplund et al. 2005), we find that our measured mass loss rate based on the detection of radio emission is in line with the \dot{M} values for Wolf-Rayet stars. The progenitors of SN 1998bw and SN 2002ap were massive stars with $M \sim 30-35$ and $20-25 M_{\odot}$, respectively, based on the optical studies. Milisavljevic et al. (2013a) places loose limits on the progenitor of SN 2012au being $< 80 M_{\odot}$.

It is contrary, however, to our current understanding that such a massive progenitor should be able to extract as much as 10^{52} erg or more from the reservoir (Burrows 1998; Fryer & Woosley 1998). More massive the core, more effective is the neutrino cooling which drains the energy reservoir and effectively makes the explosion weaker. Under such a situation, as has been argued by several authors (Bodenheimer & Woosley 1983; Hartmann & Woosley 1995; Woosley et al. 1999; Burrows et al. 2007), we may have to abandon the spherical explosion geometry resulting in the possibility of asymmetric explosions powered by the jets. The jet geometry and observer's orientation with respect to the jet axis could be a plausible explanation for the diversity of SNe including the large kinetic energies in optical but different radio emission properties.

7.3. Asymmetry in supernovae and SN 2012au

Some of the key features in the optical spectra of SN 2012au include the P-Cyg absorption profiles, asymmetries in the distribution of elements and their ions inferred from emission line profiles and the absence of Fe[III] in the iron plateau indicating high density of the Fe. Milisavljevic et al. (2013a) attributes these features to the intrinsic explosion asymmetry based on the comparisons with the model predictions by Chugai (2000); Maeda et al. (2002); Maeda & Nomoto (2003); Maeda et al. (2003, 2006); Mazzali et al. (2004). These models have shown that aspherical explosions can significantly modify both, the density profiles and distribution of elements within the ejecta.

Among the global optical properties of SN 2012au, the most distinct is the slow spectroscopic and photometric evolution similar to that in SN 1997dq and SN 1997ef (Mazzali et al. 2004), which were SN 1998bw like supernovae classified as ‘‘hypernovae’’. The spherical hydrodynamic models which describe the early light curves rather well of such energetic SNe produce fainter optical luminosities during the late linear decline phase. The two-component models which use a dense inner core in addition to the usual outer core reproduce the late linear decline phase (Chugai 2000; Maeda & Nomoto 2003). A similar explanation has been invoked by Milisavljevic et al. (2013a) in order to explain late-time emission properties of SN 2012au. The dense core required to explain these properties is also a necessary feature of the jet driven asymmetric SNe models.

Although it would be difficult to find signatures of aspherical explosion in a SN, the relative high velocity

of the shock wave could be one of those as aspherical explosion is more likely to produce anisotropic velocity distribution of the shock waves than a spherical explosion. The velocity of the shock front that is powering the synchrotron radiation and thus the radio brightness of SN 2012au is estimated to be $v = 0.2c$. This places SN 2012au among the faster shock fronts in supernovae.

7.4. Energy as a function of velocity for GRBs and SNe Ib/c

Radio synchrotron emission in supernovae is generated primarily by the electrons heated to relativistic temperatures behind the shock wave. Thus radio observations serve as a probe of high velocity ejecta. Optical observations, on the other hand, probe the slowest ejecta in the explosion, which carry most of the mass and therefore kinetic energy ($E_K = 0.3 M_{ej} v_{ej}^2 \approx 10^{51}$ erg).

In Figure 5 we compare different types of stellar explosions: GRBs and supernovae Ib/c. Standard hydrodynamic collapse results in kinetic energy profile $E_K \propto (\Gamma\beta)^{-5.2}$ shown by the solid black line (Matzner & McKee 1999). Therefore, much of the kinetic energy is deposited in the slowly moving ejecta, leaving the high velocity or mildly relativistic ejecta with negligible amount of kinetic energy, in comparison. GRBs, however, have comparable amounts of energy in slow as well as relativistic ejecta, which also points to the presence of a different source of energy - the central engine.

The kinetic energy profile of SN 2012au resembles closely to that expected from the hydrodynamic collapse and to the absence of any central engine activity. Despite the faster shock wave, the radio emission from SN 2012au conforms to the simple picture of core collapse supernovae.

8. CONCLUSIONS

SN 2012au displayed bright radio emission comparable to some of the brightest core collapse SNe. It is also one of the most energetic supernova based on the energy estimates from optical luminosities and appears to form a link between SLSN and normal core-collapse supernovae. These properties make it an important SN to shed light on the diversity among the core collapse SNe.

The smooth evolution of the radio brightness of SN 2012au over a wide range of frequency and time has been very well explained in terms of synchrotron emission from the shock that is interacting with the stellar wind of the progenitor. Based on the detailed analysis of the radio emission we infer non-relativistic velocity for the shock wave of $v \approx 0.2c$ and a moderate mass loss rate of $\dot{M} = 3.6 \times 10^{-6} M_{\odot} \text{ yr}^{-1}$ for the constant wind velocity of 1000 km/s. We estimate the internal energy associated with the shock wave to be $E \approx 10^{47}$ erg. The light curves of SN 2012au showed no sharp features or discontinuities, indicating that the shock wave did not interact with any such shells out to distance of $r \approx 10^{17}$ cm from the supernova site. Thus, the progenitor did not have such outbursts during the last few decades before the supernova.

The kinetic energy estimate from optical light curves ($E_K \approx 10^{52}$ erg) and expansion velocity makes SN 2012au an energetic event resembling SN 1998bw and SN 2002ap. SN 1998bw was associated with the

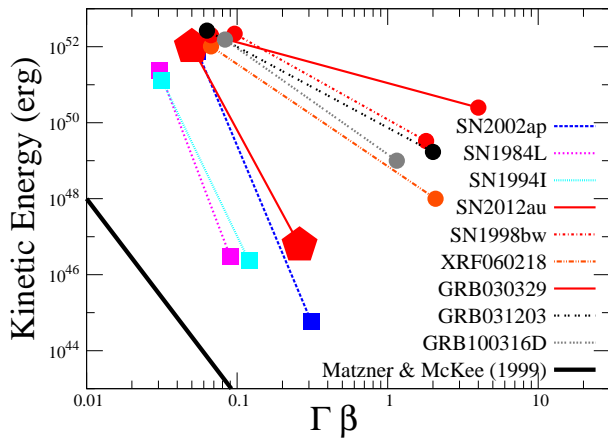


FIG. 5.— Energy as a function of velocity for GRBs and SNe Ib/c. The kinetic energy profile due to standard hydrodynamic collapse is shown as a solid black line. The high velocity ejecta of SN 2012au closely resembles the normal SNe, therefore marking it as a standard event. ^a

^aReferences: Schlegel & Kirshner (1989); Swartz & Wheeler (1991); Baron et al. (1993); Iwamoto et al. (1994); Young et al. (1995); Richmond et al. (1996); Iwamoto et al. (1998); Kulkarni et al. (1998); Höflich et al. (1999); Matzner & McKee (1999); Mil-lard et al. (1999); Woosley et al. (1999); Sollerman et al. (2000); Matheson et al. (2001); Nakamura et al. (2001); Berger et al. (2002); Mazzali et al. (2002); Berger et al. (2003b,a); Mazzali et al. (2006); Soderberg et al. (2006); Milisavljevic et al. (2013a); Margutti (2013)

GRB980425 and had the internal energy budget of 10^{49} erg for the radio emitting relativistic ejecta. SN 2002ap on the other hand had a very low energy budget of only 10^{45} erg as inferred from the radio observations. SN 2012au is intermediate - about 100 times more energetic than SN 2002ap and less energetic than SN 1998bw by the same factor. This difference in the energy budget may also be the reason for the differences in luminosities.

SN 2012au was an energetic supernova with a rare combination of properties shared by subsets of hydrogen poor hypernovae and super-luminous supernovae. These properties include high kinetic energies ($\sim 10^{52}$ erg), slow evolution, and late time optical spectral features potentially associated with explosion asymmetries.

We show that the radio emission from SN2012au is best explained by a simple model of shock interaction with a steady wind. We conclude that the unusual demise of the progenitor star was a result of the explosion properties.

Support for this work was provided by the David and Lucile Packard Foundation Fellowship for Science and Engineering awarded to AMS.

REFERENCES

- Asplund, M., Grevesse, N., & Sauval, A. J. 2005, in *Astronomical Society of the Pacific Conference Series*, Vol. 336, *Cosmic Abundances as Records of Stellar Evolution and Nucleosynthesis*, ed. T. G. Barnes, III & F. N. Bash, 25
- Barkat, Z., Rakavy, G., & Sack, N. 1967, *Physical Review Letters*, 18, 379
- Baron, E., Young, T. R., & Branch, D. 1993, *ApJ*, 409, 417
- Berger, E., Kulkarni, S. R., & Chevalier, R. A. 2002, *ApJ*, 577, L5
- Berger, E., Kulkarni, S. R., Frail, D. A., & Soderberg, A. M. 2003a, *ApJ*, arXiv:astro-ph/0307228
- Berger, E., Kulkarni, S. R., Pooley, G., et al. 2003b, *Nature*, arXiv:astro-ph/0308187
- Björnsson, C.-I., & Fransson, C. 2004, *ApJ*, 605, 823
- Bodenheimer, P., & Woosley, S. E. 1983, *ApJ*, 269, 281
- Burrows, A. 1998, in *Nuclear Astrophysics*, ed. W. Hillebrandt & E. Müller, 76
- Burrows, A., Dessart, L., Livne, E., Ott, C. D., & Murphy, J. 2007, *ApJ*, 664, 416
- Burrows, D. N., Hill, J. E., Nousek, J. A., et al. 2005, *Space Sci. Rev.*, 120, 165
- Cappa, C., Goss, W. M., & van der Hucht, K. A. 2004, *AJ*, 127, 2885
- Chatzopoulos, E., & Wheeler, J. C. 2012, *ApJ*, 760, 154
- Chevalier, R. A. 1998, *ApJ*, 499, 810
- Chevalier, R. A., & Fransson, C. 2006, *ApJ*, 651, 381
- Chevalier, R. A., & Li, Z.-Y. 1999, *ApJ*, 520, L29
- Chomiuk, L., Chornock, R., Soderberg, A. M., et al. 2011, *ApJ*, 743, 114
- Chugai, N. N. 2000, *Astronomy Letters*, 26, 797
- Fryer, C. L., & Woosley, S. E. 1998, *ApJ*, 502, L9
- Gal-Yam, A. 2012, *Science*, 337, 927
- Gal-Yam, A., Mazzali, P., Ofek, E. O., et al. 2009, *Nature*, 462, 624
- Gehrels, N., Chincarini, G., Giommi, P., et al. 2004, *ApJ*, 611, 1005
- Hartmann, D. H., & Woosley, S. E. 1995, *Advances in Space Research*, 15, 143
- Höflich, P., Wheeler, J. C., & Wang, L. 1999, *ApJ*, 521, 179
- Howerton, S., Drake, A. J., Djorgovski, S. G., et al. 2012, *Central Bureau Electronic Telegrams*, 3052, 1
- Iwamoto, K., Nomoto, K., Höflich, P., et al. 1994, *ApJ*, 437, L115
- Iwamoto, K., Mazzali, P. A., Nomoto, K., et al. 1998, *Nature*, 395, 672
- Iwamoto, K., Nakamura, T., Nomoto, K., et al. 2000, *ApJ*, 534, 660
- Kalberla, P. M. W., Burton, W. B., Hartmann, D., et al. 2005, *A&A*, 440, 775
- Kulkarni, S. R., Frail, D. A., Wieringa, M. H., et al. 1998, *Nature*, 395, 663
- Li, Z.-Y., & Chevalier, R. A. 1999, *ApJ*, 526, 716
- Maeda, K., Mazzali, P. A., Deng, J., et al. 2003, *ApJ*, arXiv:astro-ph/0305182
- Maeda, K., Mazzali, P. A., & Nomoto, K. 2006, *ApJ*, 645, 1331
- Maeda, K., Nakamura, T., Nomoto, K., et al. 2002, *ApJ*, 565, 407
- Maeda, K., & Nomoto, K. 2003, *ApJ*, arXiv:astro-ph/0304172
- Margutti, R. 2013, GRB 100316D, in preparation
- Margutti, R., Soderberg, A. M., Chomiuk, L., et al. 2012, *ArXiv e-prints*, arXiv:1202.0741 [astro-ph.HE]
- Matheson, T., Filippenko, A. V., Li, W., Leonard, D. C., & Shields, J. C. 2001, *AJ*, 121, 1648
- Matzner, C. D., & McKee, C. F. 1999, *ApJ*, 510, 379
- Mazzali, P. A., Deng, J., Maeda, K., et al. 2004, *ApJ*, 614, 858
- Mazzali, P. A., Iwamoto, K., & Nomoto, K. 2000, *ApJ*, 545, 407
- Mazzali, P. A., Nomoto, K., Patat, F., & Maeda, K. 2001, *ApJ*, 559, 1047
- Mazzali, P. A., Deng, J., Maeda, K., et al. 2002, *ApJ*, 572, L61
- Mazzali, P. A., Deng, J., Nomoto, K., et al. 2006, *Nature*, 442, 1018
- Medvedev, M. V. 2006, *ApJ*, 651, L9
- Milisavljevic, D., Soderberg, A., Margutti, R., et al. 2013a, *ArXiv e-prints*, arXiv:1304.0095 [astro-ph.HE]

TABLE 2

MODEL PARAMETERS OF SOME HYPERNOVA CANDIDATES.

References : (1) KULKARNI ET AL. (1998); (2) LI & CHEVALIER (1999); (3) MAZZALI ET AL. (2001); (4) IWAMOTO ET AL. (1998); (5) BERGER ET AL. (2002); (6) MAZZALI ET AL. (2002); (7) IWAMOTO ET AL. (2000); (8) MAZZALI ET AL. (2000); (9) MAZZALI ET AL. (2004); (10) MILISAVLJEVIC ET AL. (2013A); (11) THIS WORK

SN	ν_p	$L\nu_p$	T_p	θ_{ep}	r_{ep}	E_{ep}	B_{ep}	$\gamma \beta$	\dot{M}	T_{rise}	M_{Ni}	M_{ej}	E_k	Ref
...	GHz	erg/s-Hz	days	μ arc-sec	cm	erg	G	...	$10^{-6} M_\odot/yr$	days	M_\odot	M_\odot	10^{51} erg	...
1998bw	6	7×10^{28}	16	100	5.7×10^{16}	10^{49}	0.4	1.8	0.25	15.3	0.4	13	20	1,2,3,4
2002ap	1.4	2×10^{25}	7	40	5.4×10^{15}	10^{45}	0.2	0.31	0.5	...	0.07	2.5-5	4-10	5,6
1997ef	0.16	8	20	7,8
1997dq	0.16	...	20	9
2012au	8	7×10^{27}	20	39	1.4×10^{16}	10^{47}	0.4	0.26	3.6	16.5	0.3	3-5	10	10,11

Millard, J., Branch, D., Baron, E., et al. 1999, ApJ, 527, 746
 Moretti, A., Campana, S., Mineo, T., et al. 2005, in Society of Photo-Optical Instrumentation Engineers (SPIE) Conference Series, Vol. 5898, Society of Photo-Optical Instrumentation Engineers (SPIE) Conference Series, ed. O. H. W. Siegmund, 360
 Nakamura, T., Mazzali, P. A., Nomoto, K., & Iwamoto, K. 2001, ApJ, 550, 991
 Nomoto, K., Tominaga, N., Tanaka, M., Maeda, K., & Umeda, H. 2007, in American Institute of Physics Conference Series, Vol. 937, Supernova 1987A: 20 Years After: Supernovae and Gamma-Ray Bursters, ed. S. Immler, K. Weiler, & R. McCray, 412
 Ofek, E. O., Cameron, P. B., Kasliwal, M. M., et al. 2007, ApJ, 659, L13
 Quimby, R. M., Kulkarni, S. R., Kasliwal, M. M., et al. 2011, Nature, 474, 487
 Richmond, M. W., van Dyk, S. D., Ho, W., et al. 1996, AJ, 111, 327
 Rybicki, G. B., & Lightman, A. P. 1979, Radiative processes in astrophysics (New York, Wiley-Interscience, 1979. 393 p.)
 Schlegel, E. M., & Kirshner, R. P. 1989, AJ, 98, 577
 Smith, N., Li, W., Foley, R. J., et al. 2007, ApJ, 666, 1116

Soderberg, A. M., Kulkarni, S. R., Berger, E., et al. 2005, ApJ, 621, 908
 Soderberg, A. M., Nakar, E., Berger, E., & Kulkarni, S. R. 2006, ApJ, 638, 930
 Soderberg, A. M., Chakraborti, S., Pignata, G., et al. 2010, Nature, 463, 513
 Sollerman, J., Kozma, C., Fransson, C., et al. 2000, ApJ, 537, L127
 Swartz, D. A., & Wheeler, J. C. 1991, ApJ, 379, L13
 Takaki, K., Kawabata, K. S., Yamanaka, M., et al. 2013, ArXiv e-prints, arXiv:1306.5490 [astro-ph.HE]
 Theureau, G., Hanski, M. O., Coudreau, N., Hallet, N., & Martin, J.-M. 2007, A&A, 465, 71
 Weiler, K. W., Panagia, N., Montes, M. J., & Sramek, R. A. 2002, ARA&A, 40, 387
 Woosley, S. E., Eastman, R. G., & Schmidt, B. P. 1999, ApJ, 516, 788
 Young, D. R., Smartt, S. J., Valenti, S., et al. 2010, A&A, 512, A70
 Young, T. R., Baron, E., & Branch, D. 1995, ApJ, 449, L51

APPENDIX

THE MODEL

The supernova explosion drives a shock wave expanding into the surrounding medium that has been modified by the wind driven by the exploding star over its lifetime. The shock-wave sweeps the surrounding medium and heats it to relativistic temperatures and in the process converts the bulk kinetic energy of the incoming material into thermal energy of the shocked material. The electrons in the shock-heated plasma are accelerated in the post-shock magnetic field to radiate synchrotron radiation. Below we derive the expected flux density evolution. This model, which has been adopted from the formalism of Chevalier (1998); Soderberg et al. (2005); Chevalier & Fransson (2006), is presented here for the purpose of clarity and self-containedness.

The Electron energy distribution

We adopt a power law Lorentz factor distribution of shocked electrons with index p , as expected from the Fermi acceleration process in strong shocks:

$$n_e(\gamma_e) d\gamma_e = K_e \gamma_e^{-p} d\gamma_e \quad (\text{A1})$$

for $\gamma_m \ll \gamma_e \ll \gamma_u$, where γ_m and γ_u are the lower and upper energy cut-offs of the distribution and γ_e the electron Lorentz factors. The value of γ_m and K_e can then be found by assuming that the radiating electrons are concentrated in a thin static shell, have the non-thermal energy distribution and that the amount of energy available for the electron acceleration is a constant fraction (ϵ_e) of the total thermal energy density U_{th} .

$$\int_{\gamma_m}^{\gamma_u} n_e(\gamma_e) d\gamma_e = 4n \quad (\text{A2})$$

$$\int_{\gamma_m}^{\gamma_u} \gamma_e m_e c^2 n_e(\gamma_e) d\gamma_e = \epsilon_e U_{th} \quad (\text{A3})$$

Shock wave efficiently converts its kinetic energy into internal energy of the shocked material. For a shock wave moving several times faster than the local sound speed density compression of factor 4 is achieved and the compressed medium

trails the shock wave with speed lower by that factor. Further, it can be shown that the thermal energy density of the shocked medium is given by $U_{th} = (9/8)nm_p\beta^2c^2$. Using Eqn. A1, A2, A3 and assuming $\gamma_u \gg \gamma_m$ one obtains

$$\gamma_m = \epsilon_e \frac{9}{32} \frac{m_p}{m_e} \frac{p-2}{p-1} \beta^2 \quad (\text{A4})$$

$$K_e = 4n(p-1)\gamma_m^{p-1} \quad (\text{A5})$$

Post-shock magnetic field

It is assumed that similar to ϵ_e a fraction ϵ_B of the post-shock thermal energy goes into the magnetic field.

$$\frac{B^2}{8\pi} = \epsilon_B U_{th} \quad (\text{A6})$$

Similar to ϵ_e , in our entire discussion we will treat ϵ_B as a constant in time.

Synchrotron Spectrum

It is assumed that the shocked electrons gyrate in the post-shock magnetic fields and radiate synchrotron radiation. In order to characterize the spectrum we use the standard synchrotron formalism described in Rybicki & Lightman (1979). The radio emission spectrum could be characterized by two break frequencies and the spectral peak. The two break frequencies, corresponding to the minimum Lorentz factor of electrons (ν_m) and synchrotron self-absorption (ν_a), and the spectral peak (F_{ν_m}) are derived below.

Minimum Lorentz factor γ_m and the corresponding spectral break

The power-law distribution of the electrons has a lower Lorentz factor cut-off which we identify as γ_m (Equation A4). We adopt expression by Rybicki & Lightman (1979) for the characteristic synchrotron frequency corresponding to γ_m ,

$$\nu_m = \frac{3}{4\pi} \frac{\gamma_m^2 q B}{m_e c} \quad (\text{A7})$$

where q is the electric charge, m_e is the mass of electron.

Spectral break due to synchrotron self absorption

By approximating the thickness of the shocked radiating plasma to be $dr = r/\eta$ the optical depth can be approximated as $\tau_\nu \sim 4\alpha_\nu dr$. For the synchrotron self-absorption coefficient α_ν , we used equation 6.53 of Rybicki & Lightman (1979) and inverted the relation $\tau_\nu = 1.0$ to obtain the self-absorption frequency

$$\nu_a = \frac{1}{m_e c} 2^{\frac{2-p}{p+4}} 3^{\frac{p+1}{p+4}} \pi^{-\frac{p+2}{p+4}} q^{\frac{p+6}{p+4}} (p-1)^{\frac{2}{p+4}} B^{\frac{p+2}{p+4}} n^{\frac{2}{p+4}} \gamma_m^{\frac{2(p-1)}{p+4}} (r/\eta)^{\frac{2}{p+4}} \Gamma(x_1)^{\frac{2}{p+4}} \Gamma(x_2)^{\frac{2}{p+4}} \quad (\text{A8})$$

where $\Gamma(x_1)$ and $\Gamma(x_2)$ are the Gamma functions with $x_1 = (p/4 + 1/6)$ and $x_2 = (p/4 + 11/6)$.

Spectral Brightness

The observed flux at a luminosity distance d_L from a source of specific intensity I_ν is obtained by integrating over all solid angles: $f_\nu = \int I_\nu(\theta) \cos\theta d\Omega$ and could be well approximated as $f_\nu \simeq (j_\nu/\alpha_\nu)\Omega$ where $j_\nu = P_\nu/4\pi$ is the emissivity of an isotropic emitter and α_ν is the synchrotron self-absorption coefficient. This gives

$$f_\nu \simeq \frac{1}{4\pi} \left(\frac{P_\nu}{\alpha_\nu} \right) \Omega \quad (\text{A9})$$

Following Rybicki & Lightman (1979) the synchrotron power per unit frequency emitted by a relativistic electron is given by

$$P_\nu(\nu, \gamma) = \frac{\sqrt{3}}{2\pi} \frac{q^3 B}{m_e c^2} F \left[\frac{\nu}{\nu_{crit}(B, \gamma)} \right] \quad (\text{A10})$$

where critical frequency is defined as

$$\nu_{crit} = \frac{3x_p}{4\pi} \frac{\gamma_m^2 q B}{m_e c} \quad (\text{A11})$$

and $F(x)$ is the synchrotron function discussed in Rybicki & Lightman (1979) [see Figure 6 and Equations 6.34 of Rybicki & Lightman 1979]. For a power-law Lorentz factor distribution of electrons, Eqn. A1, power per unit volume per unit frequency $P_\nu(\nu, \gamma)$ is given by

$$P_\nu(\nu, \gamma) = \frac{\sqrt{3}}{2\pi} \frac{q^3 K_e B}{m_e c^2 (p+1)} \Gamma(x_3) \Gamma(x_4) \left(\frac{2\pi m_e c \nu}{3qB} \right)^{-(p-1)/2} \quad (\text{A12})$$

and $x_3 = (p/4 + 19/12)$, $x_4 = (p/4 - 1/12)$ [Equation 6.36 of Rybicki & Lightman 1979].

Spectral Evolution

The density profile of the surrounding medium which the shock-wave is ploughing through plays an important role in dictating the dynamics of its evolution and subsequently that of the radiation spectrum. There is a strong evidence that massive stars are the progenitors of radio SNe of Type Ib/c . Therefore the SN generated shock-wave should be expanding into the stellar wind of the progenitor star ($\rho = Ar^{-2}$). Considering this we calculate the spectral and temporal evolution in wind circumburst environment below which can be easily generalized to a different density profile. In what follows, we parameterize the wind density profile by $A = \dot{M}/4\pi V_w = 5 \times 10^{11} A_\star \text{ g cm}^{-1}$ using the mass loss rate $\dot{M} = 10^{-5} M_\odot/\text{yr}$ and wind velocity $V_w = 1000 \text{ km/s}$ (Chevalier & Li 1999).

The instantaneous synchrotron spectrum can then be characterized by two break frequencies (ν_a and ν_m) and the spectral peak F_m . Usually, however, the peak frequency ν_m is below observing band and therefore the spectral peak is rarely observed in SNe. We therefore express it in terms of an observable f_{ν_a} or the flux at the self-absorption frequency which is related to the spectral peak $f_{\nu_a} = F_m(\nu_a/\nu_m)^{-(p-1)/2}$. Because the shock wave, and therefore the radiating plasma behind it, is expected to be moving at non-relativistic or mildly relativistic velocities we have neglected relativistic effects including doppler boosting, for simplicity. Equations A4-A12 then give

$$\nu_m \approx 7 \times 10^4 q \frac{m_p^2}{m_e^3} \left(\frac{p-2}{p-1} \right)^2 \sqrt{A_\star} \sqrt{\epsilon_B} \epsilon_e^2 \frac{\beta^5}{r} \text{ Hz} \quad (\text{A13})$$

$$f_{\nu_a} \approx 8 \times 10^{11} q^{\frac{p(1.1p+62.6)+89.8}{p+4}} c^{-\frac{1}{2}} c^{\frac{5(p/2+1)}{p+4}} m_p^{\frac{5p-5}{p+4}} m_e^{\frac{11-3.5p}{p+4}} f_p f_\Gamma A_\star^{\frac{p+6.5}{p+4}} \beta^{\frac{12p-7}{p+4}} \eta^{-\frac{5}{p+4}} \epsilon_B^{\frac{p+1.5}{p+4}} \epsilon_e^{\frac{5p-5}{p+4}} d_{L,100}^{-2} \text{ mJy} \quad (\text{A14})$$

along with the synchrotron self absorption frequency

$$\nu_a = 5 \times 10^{40} q^{\frac{38.8+28.5p}{p+4}} c^{\frac{p+2}{p+4}} \left(\frac{m_e}{m_p} \right)^{\frac{-2(p-1)}{p+4}} \left[\frac{p-2}{p-1} \right]^{\frac{2(p-1)}{p+4}} (p-1)^{\frac{2}{p+4}} A_\star^{\frac{3+p/2}{p+4}} \beta^{\frac{5p-2}{p+4}} \frac{p/2+1}{r} \epsilon_B^{\frac{p/2+1}{p+4}} \epsilon_e^{\frac{2(p-1)}{p+4}} \eta_{12}^{-\frac{2}{p+4}} \Gamma^{\frac{2}{p+4}}(x_3) \Gamma^{\frac{2}{p+4}}(x_4) \text{ Hz} \quad (\text{A15})$$

where $f_p = \left(\frac{p-2}{p-1} \right)^{\frac{5.5p-5}{p+4}} \frac{(p-1)^{\frac{5}{p+4}}}{p+1}$ and $f_\Gamma = \Gamma(x_1)\Gamma(x_2)\Gamma^{-\frac{p-1}{p+4}}(x_3)\Gamma^{-\frac{p-1}{p+4}}(x_4)$, and $d_{L,100}$ to be the luminosity distance in units of 100 Mpc.